Bile acids increase intestinal markers via FXR/SNAI2/miR-1 axis in the stomach

Na Wang
The Forth Military Medical University, State Key Laborary of Cancer Biology, Xijing Hospital of Digestive Diseases

Min Chen
The Forth Military Medical University, State Key Laborary of Digestive Diseases, Xijing Hospital of Digestive Diseases

Jiaoxia Zeng
The Forth Military Medical University, State Key Laborary of Cancer Biology, Xijing Hospital of Digestive Diseases

Guofang Lu
The Forth Military Medical University, State Key Laborary of Cancer Biology, Xijing Hospital of Digestive Diseases

Jiaojiao Wang
Shaanxi University of Chinese Medicine

Jian Zhang
The Forth Military Medical University, State Key Laborary of Digestive Diseases, Xijing Hospital of Digestive Diseases

Siran Wu
The Forth Military Medical University, State Key Laborary of Digestive Diseases, Xijing Hospital of Digestive Diseases

Yongquan Shi (shiyquan@fmmu.edu.cn)
Fourth Military Medical University https://orcid.org/0000-0001-9515-7577

Primary research

Keywords: Intestinal metaplasia, Gastric cancer, FXR, SNAI2, CDX2

Posted Date: May 15th, 2020

DOI: https://doi.org/10.21203/rs.3.rs-27417/v1

Abstract

Background

Intestinal metaplasia (IM) is a precancerous lesion that increases risk of subsequent gastric cancer (GC). However, factors governing the transformation from normal gastric epithelial cells to IM remain unclear. Previously, miR-1 turned out to play an essential role in the initiation of bile acids (BA)-induced IM. Here, we investigate the mechanism underlying miR-1 inhibition by BA in gastric cells.

Methods

We conducted IPA analysis to determine the potential molecular interacting BA with miR-1. The changes of FXR and SNAI2 after BA treatment were detected by western blot and qRT-PCR. IHC was performed to assess the expression level of FXR and SNAI2 in normal and IM tissue microarrays. The transcriptional regulation of SNAI2 or miR-1 was verified by bioinfamatics, luciferase reporter assay and chromatin immunoprecipitation PCR.

Results

BA treatment caused aberrant expression of FXR and IM markers in gastric cells. Augmented FXR led to the transcriptional activation of SNAI2 which further stimulates the expression of downstream IM markers. Bioinformatics analysis indicated that SNAI2 had miR-1 promoter binding region and we identified that SNAI2 negatively regulated miR-1 transcription. Both FXR and SNAI2 were increased in patients with IM.

Conclusions

This study demonstrated that FXR might be responsible for a series molecular changes in gastric cells after BA, and FXR/SNAI2/miR-1 axis exert a crucial role in BA-induced IM progression. Blocking the activation of the FXR-oriented axis may provide a promising approach for IM or even GC treatment.

Background

Gastric cancer is the fifth most common malignant tumor but the third leading cause of cancer-related death worldwide [1]. We gradually recognized that gastric IM is one of the most common precancerous lesions of intestinal-type GC which follows the development model from chronic atrophic gastritis, IM, atypical hyperplasia and then to GC [2, 3]. Preventing the development of IM may block the arising of intestinal-type GC. However, the mechanism underlying the occurrence of IM in gastric mucosa is far from clear.

It is generally believed that chronic environmental stimulation leads to gastric IM, such as *Helicobacter pylori (Hp)* infection and bile acids (BA) reflux [4, 5]. However, whether *Hp* eradication could prevent the occurrence or further development of gastric cancer is still controversial [6, 7], indicating other factors may contribute to the development of IM. BA is one kind of the important factors inducing or exacerbating IM [8]. Interestingly, a large number of studies have shown that BA stimulation could cause IM in the esophagus and the mechanism of its occurrence have been largely revealed [9–12]. However, there are few studies on the mechanism underlying the prometalpastic role of BA in gastric cells. According to clinical statistical results, the risk of gastric IM in patients with bile reflux is 11 times higher than that in patients without bile reflux [13]. However, the mechanism of BA promoting gastric IM remains to be further studied.

MicroRNAs (miRNAs) causes the degradation of mRNA or the inhibition of translation by binding the 3'noncoding region (3'-UTR) of the target gene messenger RNA (mRNA) and play important roles in regulating biologic processes of cells [14, 15]. At present, many studies have provided evidence that miRNAs participate in the development, differentiation and formation of the digestive tract, so it also exert great influence in the occurrence of IM, such as miR-30, miR-194 and miR-490 [16, 17]. Moreover, it should be noted that our team has successfully constructed a cell model of BA-induced gastric IM, and found that miR-92 promotes the expression of IM markers Caudal-related homeobox 2 (CDX2), Krüppel-like factor 4 (KLF4) and VILLIN 1 (VIL1) by targeting FOXD1 [18]. We also discovered that miR-1 was significantly reduced in tissues of patients with IM and cell models of BA-induced IM, as well as the reduction of which promoted the significant increase of CDX2, MUC2, KLF4 via targeting both HDAC6 and HNF4α (manuscript submitted for publication). But, the mechanism of miR-1 depression triggered by BA remains to be elucidated. In the current study, we performed IPA analysis between miR-1 and BA potential receptor Farnesoid X Receptor (FXR, also known as NR1H4), Takeda G-coupled Protein Receptor 5 (TGR5), Small Heterodimer Partner (SHP), Constitutive and Rostane Receptor (CAR) and Vitamin D Receptor (VDR), and the results suggested that FXR might be the interacting protein.

FXR, BA activated receptor, is expressed in intestine and liver predominantly to maintain BA homeostasis [19, 20]. FXR can also serve as a transcription factor to regulate the expression of downstream genes by directly binding to their promoter. With the increasing recognition of the important role of BA in the induction of IM of gastric mucosa, researchers began to study the role of FXR in this process. Yu JH et al. found that upregulation of CDX2 and MUC2 in BA-induced gastric IM cells resulted from activated FXR/NF-κB pathway [21]. Similarly, one of our previous studies found that FXR is responsible for the enhancement of CDX2 by a SHP-dependent way in gastric cells [22]. However, the study on the mechanisms of FXR promotes BA-induced gastric IM is still far from enough.

Herein, we identified that FXR/SNAI2/miR-1 axis was dramatically activated in gastric cells after BA treatment and triggered an intestinal-like phenotype. Based on our results and recent findings suggesting the role of FXR in IM and tumor, we hypothesized that FXR may be responsible for the molecular changes result from BA stimulation and facilitate succeeding progression of IM and GC.

Methods

Cell lines

The BA-induced IM cell model was described previously [18]. GES-1 and AGS (purchased from ATCC) were cultured in PRIM-1640 medium (Gibco, USA) with 10% fetal bovine serum (Gibco, USA), 100 mg/ml streptomycin and 100 U/ml penicillin. The primary cells were incubated in ICell Primary Epithelial Cell Culture System (icellbioscience, China) with 2% fetal bovine serum (Biocytosci, USA). Deoxycholic acid (DCA) was chosen for the following experiments as it is a major hydrophobic bile acid with potent cytotoxicity (BiocytoSci, USA).

Tissue microarray and human IM samples

A normal tissue microarray containing 24 cases (BN01011b) and a gastric IM tissue microarray (ST8017a) containing 80 cases of gastric IM cases were purchased from Alenabio Biotech (China). Ten paired human gastric IM specimens were obtained from patients who underwent gastroscopy. The pathological data of these specimens was collected from the Department of Pathology. Our study was approved by the ethics committee of Xijing Hospital. All patients signed informed consent before the specimens were obtained. To exclude the effect of *Hp* infection, all of the patients we selected were *Hp* negative.

Immunohistochemistry

Immunohistochemistry (IHC) was performed using anti-FXR (1:50, abcam, #187735), anti-SNAI2 (1:50, Invitrogen, #PA5-73015) antibodies following the manufacturer's instructions. The IHC results were independently evaluated by two professional pathologists independently. The scoring was the product of positive rate and intensity of staining. Staining intensity: negative (0), weak (1), moderate (2), and strong (3). The positive rate of staining: <10% (0), 10%-25% (1), 26%-50% (2), 51%-75(3), and >75% (4).

Immunofluorescence

Cells were plated in 4-well chamber slides (Millipore, USA). Then, the cells were washed by twice with cold PBS, fixed with 500μl of 4% paraformaldehyde for 35 minutes, permeabilized with 200μl 1% Triton X-100, for 10 minutes and blocked with 500μl of goat serum, for 30 minutes. Then the cells were incubated with primary antibodies at 4°C overnight. Then the cells were incubated with the FITC secondary antibody at room temperature for 2 hours. Finally, the nuclei were stained with DAPI (Solarbio) for 10 minutes. IF staining for FXR was performed in GES-1 cells. The primary antibodies were a rabbit anti-human FXR antibody (1:100, abcam, #187735).

RNA extraction and real-time PCR

TRIzol® reagent (Invitrogen, USA) was used to extract the total RNA from cell lines and human tissue samples according to a standard protocol. Then RNA was reverse transcribed into cDNA using the

PrimeScript® RT Reagent kit (Takara Biotechnology, Japan) at 37˚C for 15 minutes and 85˚C for 5 seconds, followed by temperature maintenance at 4˚C. And qPCR was conducted using SYBR Premix Ex Taq II (Takara Biotechnology, Japan) on a CFX96™ Real-Time PCR Detection system (Bio-Rad Laboratories, USA). β-actin and U6 were used as the internal control and the $2^{\Delta\Delta Cq}$ method was utilized to quantify the relative mRNA expression of each gene. Sequences of gene-specific primers are shown in Table 3.

Protein extraction and western blot analysis

Total protein was extracted by mixing cells with radioimmunoprecipitation assay (RIPA) buffer (Beyotime, China), which was supplemented with protease and phosphatase inhibitors. Western blot analysis was carried out following standard procedures. The following antibodies were used for this experiment: anti-FXR (1:200, abcam, #187735), anti-SNAI2 (1:1000, abcam, #106077), anti-HDAC6 (1:1000, Cell Signaling Technology, #7558), anti-HNF4α (1:2000, Abcam, #92378), anti-CDX2 (1:1000, Cell Signaling Technology, #12306), and anti-β-actin (1:5000, Bioworld, #AP0060). The primary antibody dilution buffer, PREstain Protein Ladder and Western SuperSensitive Substrate were purchased from BioCytoSci (USA).

Transfection

Synthetic miR-1 agomir, the corresponding negative control oligonucleotides and plasmid small interfering RNA (siRNA) were purchased from Genepharma (China), and the sequence of them was shown in Table 4. Attractene transfection reagent was added to Opti-MEM to generate the transfection medium. Cells were cultured in the transfection medium and it was replaced with fresh medium after 6 hours. Then the cells were grown in 5% CO_2 at 37°C for an additional 48 hours. The transfection regent was purchased from Thermo Fisher Scientific (USA) and was used following the manufacturer's protocol. SNAI2 and FXR overexpression lentiviral vector were designed and provided by Genechem Co. Ltd. (China). GES-1 cells were infected with the lentivirus for 48 hours and then cultured with 2 μg/ml puromycin for 7 days.

Dual-luciferase report assay

We amplified a specific sequence upstream of the transcription start sites of the SNAI2 promoter by PCR, and then cloned it into a pGL3-basic luciferase vector (Invitrogen, USA) to generate SNAI2-p1 (-2000bp~+500bp), SNAI2-p2 (-543bp~+500bp), SNAI2-p3 (+398bp~+500bp) and SNAI2-p4 (+415bp~+500bp). We also amplified the 2000 bp sequence upstream of the transcription start sites of the miR-1 promoter, and then cloned it into the pGL3-basic luciferase vector.

Chromatin immunoprecipitation

GES-1 cells were transiently transfected with a miR-1 promoter vector. Then, ChIP analysis was performed according to the standard method of the Magna ChIP G Assay kit (Millipore, USA). Chromatin was immunoprecipitated with anti-FXR, anti-SNAI2 or the negative control IgG. Finally, immunoprecipitated

DNA-protein complexes were isolated and a real-time PCR assay was carried out to examine the quantity of specific proteins. The primers for the SNAI2 and miR-1 promoters are listed in Table 3.

Statistical analysis

The SPSS software (V.19.0, SPSS, USA) statistical package was used to conduct all statistical analyses. All continuous data are expressed as the mean±SD. The χ^2 test was used to compare the frequencies of categorical variables. Mutual associations among clinical results were assessed by using Spearman's rank correlation. Statistical comparisons between two groups were analyzed with unpaired Student's t test. P values less than 0.05 were considered statistically significant.

Results

FXR expression is increased in intestinal metaplastic cells

In our previous study, decreased miR-1 was found to promote the transformation from normal gastric cells to IM cells after BA through targeting both HDAC6 and HNF4α. To uncover the mechanism by which BA inhibiting miR-1, we conducted IPA data analysis which showed that FXR might correlate BA with miR-1 (Fig. 1a). Then, we examined the protein levels of FXR in GES-1 cells treated with DCA (100μM) for 24 hours. As expected, DCA caused the increase of FXR along with the high expression of CDX2, KLF4 and MUC2 (Fig. 1b). Next, because of the deficiency in the mouse model with bile reflux, we attempted to utilize Sprague-Dawley (SD) rat primary gastric epithelial cells suffered from DCA to mimic the condition. Similarly, the result showed that FXR and intestinal markers were enhanced in primary cultured cells after DCA (Fig. 1c). In addition, IF staining for FXR was performed in GES-1 cells and the results reconfirmed that DCA caused the enhancement of FXR in gastric cells (Fig. S1a). These results indicated that FXR might participate in the downstream activation induced by BA.

Further, to determine the significance of FXR in IM tissues of patients, we detected and analyzed its expression level in IM and normal tissues. Besides, high expression of FXR was observed more frequently in IM tissues and mainly located in the nucleus (Fig. 1d, 1e, Table 1). Moreover, the correlation analysis showed that the expression of FXR was negatively related to miR-1 ($r = -0.2390$, $p = 0.0328$) and positively correlated with target molecules HDAC6 ($r = 0.4959$, $p = 0.0001$) and HNF4α ($r = 0.7665$, $p = 0.0001$) of miR-1 (Fig. S1b, 1f, 1g) in IM tissues. Additionally, mRNA level of FXR was found to be higher in IM tissue cells Compared with normal tissues (Fig. 1h). Collectively, these results suggested that FXR might involve in the occurrence and development of IM.

FXR regulates downstream IM markers and miR-1

We used loss-of-function and gain-of-function experiments to study FXR function in regulating intestinal markers. And the results showed that the overexpression of FXR in GES-1 cells resulted in the increase of HDAC6 and HNF4α, as well as the overexpression of CDX2 (Fig. 2a). At the same time, it can be seen that the enhancement of FXR led to the downregulation of miR-1 (Fig. 2b). On the contrary, HDAC6, HNF4α

and CDX2 decreased significantly after knockdown of FXR in AGS cells (Fig. 2c). The decrease of it also caused the augment of miR-1 (Fig. 2d). Together, these results indicated that FXR could not only mediate the downstream intestinal markers and miR-1 target molecules positively, but also suppress the expression of miR-1.

SNAI2 is enhanced in BA-induced IM cells

IPA data analysis revealed that FXR might influence the expression of miR-1 through SNAI2, NCL, AKT and MET. Through bioinformatics analysis, we found that as a transcription factor, SNAI2 has the binding sites on the promoter region of miR-1. Then we detected the protein and mRNA level of SNAI2 in DCA-treated cells and found that it increased substantially, in contrast to control cells (Fig. 3a, 3b). Besides that, SNAI2 was also upregulated obviously on both protein and RNA levels in primary cells in response to DCA treatment (Fig. 3c, 3d). Moreover, it could be observed that SNAI2 was enhanced as well as positively correlated with FXR in IM tissues (Fig. 3e, 3f, 3g, Table 2). Its mRNA level was also significantly increased in IM tissues of patients in contrast to adjacent normal tissues (Fig. 3h). Collectively, these results suggested that SNAI2 was overexpressed in BA-induced IM cells.

SNAI2 is transcriptionally activated by FXR in gastric cells

To further clarify the role of FXR and SNAI2 in the process of BA-induced IM, we explored the regulatory relation between FXR and SNAI2. As showed in figure 4a, CDX2 enhancement induced by DCA could be reversed by FXR specific siRNA. After that, GES-1 cells were infected with FXR expression vector and transfected with siSNAI2 simultaneously. It can be seen that the upregulation of SNAI2 and CDX2 induced by FXR could be inversed by siSNAI2 (Fig. 4b). On the contrary, we could see that the decrease of FXR resulted in correspondingly diminishing of SNAI2 and CDX2 in AGS cells, whereas no inhibition was observed after overexpression of SNAI2 (Fig. 4c). According to the prediction results of JASPAR database (http://jaspar.binf.ku.dk/), we constructed a series of reporter gene vectors containing different sequences upstream of SNAI2 transcription starting point. The results showed that the activities of SNAI2-p1 and SNAI2-p2 were higher than other sequences without any treatment, and the transcription activity of them was significantly higher in GES-1 cells after transfected with FXR expression plasmid (Fig. 4d). The results of ChIP assays further indicated that ChIP-1(GAGGTAATTAT) sequence might be the putative binding site of FXR on SNAI2 promoter (Fig. 4e). The above results indicated that FXR could promote the transcription of SNAI2 and induce its elevation in BA-induced IM cells.

SNAI2 promotes IM by inhibiting miR-1 transcriptionally

To further uncover the mechanism of pro-metaplastic function of SNAI2, we examined its functional regulation on downstream intestinal markers and miR-1. At first, we could see that high expression of SNAI2 resulted in an evident decrease of miR-1 (Fig. 5a). Conversely, miR-1 was augmented after downregulating SNAI2 (Fig. 5b). When SNAI2 and miR-1 were overexpressed simultaneously, it could be found that miR-1 reversed the elevation of HDAC6 and HNF4α induced by SNAI2 (Fig. 5c, 5d). Furthermore, to ascertain whether SNAI2 could regulate the activity of the promoter of miR-1, we co-

transfected SNAI2 expression vector with miR-1 full-length promoter reporter gene in GES-1 cells. The results showed that SNAI2 could evidently reduce miR-1 promoter activity (Fig. 5e). Then we constructed different promoter sequences: ChIP 1 (-1660bp~-1389bp); ChIP 2 (-1205bp~-982bp); ChIP 3 (-649bp~-420bp), ChIP NC (-5930bp ~-5672bp). ChIP assays were utilized to detect the binding sites of SNAI2 to these sequences. Finally, the results showed that ChIP 1 and ChIP 2 could bind to SNAI2 promoter directly, and the combination of them was reinforced by DCA (Fig. 5f). In summary, our findings suggested that SNAI2 overexpression in BA-induced IM cells contributed to the reduction of miR-1 promoter activity and elevation of intestinal markers.

Discussion

In this study, for the first time, we identified the aberrant expression of FXR and SNAI2 in IM cells and their key roles in BA-stimulated metaplastic progression. Interestingly, SNAI2 regulated miR-1 transcription negatively which further targeted downstream intestinal markers. Therefore, FXR/SNAI2/miR-1 axis mediates the expression of intestinal markers in IM cells. In addition, the axis triggered by DCA may promote the transformation of normal gastric cells to IM cells and mediate the further development of IM to GC.

Now, the mechanism of the transformation from normal gastric mucosal cells to intestinal cells is not clear. It is widely accepted that IM is the result of the interaction of a series of intestine related transcription factors and CDX2 plays an indispensable role in stimulating intestinal differentiation [22–27]. Recently, what attracts people's attention is the regulatory mechanism of CDX2 in intestinal differentiation. In a previous study, our group confirmed that increased miR-92 is involved in the upregulation of CDX2 and the downstream IM markers in gastric cells treated by BA [18]. Besides, our in vivo and in vitro experiments provided evidence that downregulation of miR-1 facilitated the formation of a positive feedback loop involving HDAC6/HNF4α and then stimulated CDX2 expression in BA-induced IM cells. Herein, we sought to elucidate the regulatory mechanism of DCA on miR-1 and to establish a molecular network of the alterations during BA-induced gastric IM progression. GES-1, a kind of immortalized gastric cell, is regarded as a non-malignant cell line which was used to imitate gastric epithelial cells. In addition, we detected the changes of target molecules in gastric mucosa cells of SD rats treated with BA.

A retrospective prospective follow-up study conducted in Japan found that the incidence of GC in patients with high level of BA in gastric juice (≥ 1000 mmol / L) significantly higher than patients with low gastric BA level (< 1000 mmol / L) [13]. Another multicenter study also showed that the risk of GC was 2.4 times higher in the high concentration BA group than in the other groups [8]. FXR regulates the biosynthesis, secretion and transport of BA as well as participates in various metabolic diseases [28]. And it is not only the principal nuclear receptor of BA, but also a transcription factor to regulate gene transcription [29]. So we speculated that it might involve in the stimulation of BA on gastric cells. In this study, we observed that the expression level of FXR increased in IM tissues as well as in GES-1 cells and primary cultured cells after BA treatment. We also provide evidence that FXR could stimulate the

expression of downstream intestinal markers and the FXR specific siRNA could abolish the enhancement of these markers induced by DCA. Consistently, there are some studies showed evidence that FXR was augmented in intestinal-type GC with IM as well as contributed to the increase of MUC2 and CDX2 in gastric cells [30, 31]. Hence, we guess that there might be possible that FXR mediates the prometaplastic effect of DCA on gastric cells.

Based on IPA and bioinformatics analysis, SNAI2 was considered to connect FXR with miR-1. SNAI2 (also known as Slug), a member of Snail superfamily, is one of the transcription factors of epithelial mesenchymal transition (EMT) [32]. In recent years, it has been found that SNAI2 is abnormally expressed in various kinds of malignant tumors and plays an important role in tumor progress and prognosis [33–35]. To investigate the role of SNAI2 in IM cells, we examined its expression level in IM tissues and BA-induced IM cells. The results confirmed that it is positively correlated with FXR in IM tissues and could be activated by DCA in GES-1 cells as well as primary cultured cells. Further, we analyzed the sequence of SANI2 promoter and found that FXR might have binding sites on its promoter. Next, data of ChIP and luciferase reporter gene assays confirmed that FXR could directly bind to SNAI2 promoter and activate its transcription. And increased IM markers via FXR overexpression or DCA could be blocked by SNAI2 knock-down which means that it could mediate the prometaplastic function of DCA. We also provided evidence that SNAI2 could stimulate the expression of intestinal markers in gastric cells and primary cultured cells. These results are partly consistent with some studies showing that SNAI2 promotes the malignant transformation of gastric cells through an EMT dependent manner [36–39]. Nevertheless, in this study, we first identified that SNAI2 was augmented in IM tissues and could promote the expression of intestinal markers in gastric cells.

In terms of the downstream markers regulation, miR-1 was bioinfamatically identified as the functional targets of SNAI2. The dysregulation of miR-1 was proved to contribute to the aggressive progression and poor prognosis of human gastric cancer [40]. More interestingly, miR-1 was previously found to post-transcriptionally regulate SNAI2 to inhibit EMT in different kind of cancer [41, 42]. Conversely, in this study, we proved that SNAI2 directly binds to the two sites (-1205bp~ -982 bp and − 649bp~ -420 bp) on the promoter of miR-1 to inhibit its transcription. In our previous study has shown that miR-1 could target 3'UTR of both HDAC6 and HNF4α to suppress their expression. Moreover, DCA inhibited miR-1 in gastric cells to induce high expression of HDAC6 and HNF4α which stimulated intestinal markers. Together with the results here, we identified a complex signal network through witch DCA induced the arising and continuous progression of IM in the stomach. Collectively, this study, for the first time, showed evidence that BA-induced gastric IM is realized, in part, by FXR/SNAI2/miR-1 axis. However, it is noteworthy that the model systems of bile reflux, such as mouse model or primary cells from human gastric mucosa, will be needed in our future studies.

Conclusions

In summary, the findings of this study revealed a schematic model of gastric IM development (Fig. 6). This figure describes that BA induces the upregulation of FXR in gastric cells to further stimulate the

activation of SNAI2, leading to the transcriptional inhibition of miR-1, which finally promotes the transcription of downstream intestinal markers. Hence, FXR might serve as a critical regulator of BA-induced intestinal phenotype in gastric epithelial cells. This new FXR/SNIA2/miR-1 axis may provide a novel insight into the mechanism underlying the initiation and development of gastric IM. Suppression of FXR to abrogate the pathway may be a potential approach for preventing gastric IM or even GC in patients with bile regurgitation.

Abbreviations

GC: Gastric cancer; IM: Intestinal metaplasia; BA: Bile acids; DCA: deoxycholic acid; FXR: Farnesoid X Receptor.

Declarations

Ethics approval and consent to participate

All human studies were approved by the Human Subjects committee of Xijing Hospital, Xi'an China. And all patients signed the informed consent before the specimens were obtained. All animal experiments were approved by Animal Research Committee of Xijing Hospital, Xi'an China.

Consent for publication

All authors have agreed to publish this manuscript.

Availability of data and materials

All data generated or analyzed during this study are included in this manuscript.

Competing interests

The authors declare no potential conflicts of interest.

Funding

This work was supported by grants from National Natural Science Foundation of China (No. 81873554 to YQS).

Authors' contributions

All authors included in this paper fulfill the criteria of authorship and have approved the submission of this manuscript. NW, and YQS designed the experiments. NW, MC, JXZ, GFL, JJW, JZ and SRW performed the study. YQS supervised the study.

Acknowledgements

We wish to thank Zhang Lifeng and Dr. Wu qiong (Xijing Hospital of Digestive Diseases) for technical assistance.

Authors' information

[1]The Fourth Military Medical University, Xijing Hospital of Digestive Diseases, State Key Laboratory of Cancer Biology, Xi'an, 710032, China. [2]Shannxi University of Chinese Medicine, Xi'an, 712046, China.

References

1. Bray F, Ferlay J, Soerjomataram I, Siegel RL, Torre LA, Jemal A. Global cancer statistics 2018: GLOBOCAN estimates of incidence and mortality worldwide for 36 cancers in 185 countries. CA Cancer J Clin. 2018;68:394–424.
2. Sue S, Shibata W, Maeda S. Helicobacter pylori-Induced Signaling Pathways Contribute to Intestinal Metaplasia and Gastric Carcinogenesis. Biomed Res Int. 2015;2015:737621.
3. Correa P. Human gastric carcinogenesis: a multistep and multifactorial process–First American Cancer Society Award Lecture on Cancer Epidemiology and Prevention. Cancer Res. 1992;52:6735–40.
4. Dixon MF, Mapstone NP, Neville PM, Moayyedi P, Axon AT. Bile reflux gastritis and intestinal metaplasia at the cardia. Gut. 2002;51:351–5.
5. Jiang JX, Liu Q, Zhao B, Zhang HH, Sang HM, Djaleel SM, et al. Risk factors for intestinal metaplasia in a southeastern Chinese population: an analysis of 28,745 cases. J Cancer Res Clin Oncol. 2017;143:409–18.
6. Leung WK, Lin SR, Ching JY, To KF, Ng EK, Chan FK, et al. Factors predicting progression of gastric intestinal metaplasia: results of a randomised trial on Helicobacter pylori eradication. Gut. 2004;53:1244–9.
7. Lee YC, Chen TH, Chiu HM, Shun CT, Chiang H, Liu TY, et al. The benefit of mass eradication of Helicobacter pylori infection: a community-based study of gastric cancer prevention. Gut. 2013;62:676–82.
8. Matsuhisa T, Arakawa T, Watanabe T, Tokutomi T, Sakurai K, Okamura S, et al. Relation between bile acid reflux into the stomach and the risk of atrophic gastritis and intestinal metaplasia: a multicenter study of 2283 cases. Dig Endosc. 2013;25:519–25.
9. Malfertheiner P, Peitz U. The interplay between Helicobacter pylori, gastro-oesophageal reflux disease, and intestinal metaplasia. Gut. 2005;54(Suppl 1):i13–20.
10. Souza RF. The role of acid and bile reflux in oesophagitis and Barrett's metaplasia. Biochem Soc Trans. 2010;38:348–52.
11. Kazumori H, Ishihara S, Takahashi Y, Amano Y, Kinoshita Y. Roles of Kruppel-like factor 4 in oesophageal epithelial cells in Barrett's epithelium development. Gut. 2011;60:608–17.

12. Das KM, Kong Y, Bajpai M, Kulkarni D, Geng X, Mishra P, et al. Transformation of benign Barrett's epithelium by repeated acid and bile exposure over 65 weeks: a novel in vitro model. Int J Cancer. 2011;128:274–82.
13. Tatsugami M, Ito M, Tanaka S, Yoshihara M, Matsui H, Haruma K, et al. Bile acid promotes intestinal metaplasia and gastric carcinogenesis. Cancer Epidemiol Biomarkers Prev. 2012;21:2101–7.
14. Bartel DP. MicroRNAs: target recognition and regulatory functions. Cell. 2009;136:215–33.
15. Lujambio A, Lowe SW. The microcosmos of cancer. Nature. 2012;482:347–55.
16. Sousa JF, Nam KT, Petersen CP, Lee HJ, Yang HK, Kim WH, et al. miR-30-HNF4gamma and miR-194-NR2F2 regulatory networks contribute to the upregulation of metaplasia markers in the stomach. Gut. 2016;65:914–24.
17. Shen J, Xiao Z, Wu WK, Wang MH, To KF, Chen Y, et al. Epigenetic silencing of miR-490-3p reactivates the chromatin remodeler SMARCD1 to promote Helicobacter pylori-induced gastric carcinogenesis. Cancer Res. 2015;75:754–65.
18. Li T, Guo H, Li H, Jiang Y, Zhuang K, Lei C, et al. MicroRNA-92a-1-5p increases CDX2 by targeting FOXD1 in bile acids-induced gastric intestinal metaplasia. Gut. 2019;68:1751–63.
19. Forman SA, Miller KW, Yellen G. A discrete site for general anesthetics on a postsynaptic receptor. Mol Pharmacol. 1995;48:574–81.
20. Seol W, Choi HS, Moore DD. Isolation of proteins that interact specifically with the retinoid X receptor: two novel orphan receptors. Mol Endocrinol. 1995;9:72–85.
21. Yu JH, Zheng JB, Qi J, Yang K, Wu YH, Wang K, et al. Bile acids promote gastric intestinal metaplasia by upregulating CDX2 and MUC2 expression via the FXR/NF-kappaB signalling pathway. Int J Oncol. 2019;54:879–92.
22. Zhou H, Ni Z, Li T, Su L, Zhang L, Liu N, et al. Activation of FXR promotes intestinal metaplasia of gastric cells via SHP-dependent upregulation of the expression of CDX2. Oncol Lett. 2018;15:7617–24.
23. Guo RJ, Suh ER, Lynch JP. The role of Cdx proteins in intestinal development and cancer. Cancer Biol Ther. 2004;3:593–601.
24. Silberg DG, Swain GP, Suh ER, Traber PG. Cdx1 and cdx2 expression during intestinal development. Gastroenterology. 2000;119:961–71.
25. Silberg DG, Sullivan J, Kang E, Swain GP, Moffett J, Sund NJ, et al. Cdx2 ectopic expression induces gastric intestinal metaplasia in transgenic mice. Gastroenterology. 2002;122:689–96.
26. Mutoh H, Sakurai S, Satoh K, Tamada K, Kita H, Osawa H, et al. Development of gastric carcinoma from intestinal metaplasia in Cdx2-transgenic mice. Cancer Res. 2004;64:7740–7.
27. Matsuzaki J, Suzuki H, Tsugawa H, Watanabe M, Hossain S, Arai E, et al. Bile acids increase levels of microRNAs 221 and 222, leading to degradation of CDX2 during esophageal carcinogenesis. Gastroenterology. 2013;145:1300–11.

28. Matsubara T, Li F, Gonzalez FJ. FXR signaling in the enterohepatic system. Mol Cell Endocrinol. 2013;368:17–29.
29. Wang YD, Chen WD, Moore DD, Huang W. FXR: a metabolic regulator and cell protector. Cell Res. 2008;18:1087–95.
30. Lian F, Xing X, Yuan G, Schafer C, Rauser S, Walch A, et al. Farnesoid X receptor protects human and murine gastric epithelial cells against inflammation-induced damage. Biochem J. 2011;438:315–23.
31. Li S, Chen X, Zhou L, Wang BM. Farnesoid X receptor signal is involved in deoxycholic acid-induced intestinal metaplasia of normal human gastric epithelial cells. Oncol Rep. 2015;34:2674–82.
32. Chen T, You Y, Jiang H, Wang ZZ. Epithelial-mesenchymal transition (EMT): A biological process in the development, stem cell differentiation, and tumorigenesis. J Cell Physiol. 2017;232:3261–72.
33. Majorini MT, Manenti G, Mano M, De Cecco L, Conti A, Pinciroli P, et al. cIAP1 regulates the EGFR/Snai2 axis in triple-negative breast cancer cells. Cell Death Differ. 2018;25:2147–64.
34. Liu BW, Yu ZH, Chen AX, Chi JR, Ge J, Yu Y, et al. Estrogen receptor-alpha-miR-1271-SNAI2 feedback loop regulates transforming growth factor-beta-induced breast cancer progression. J Exp Clin Cancer Res. 2019;38:109.
35. Wang Y, Xiong H, Liu D, Hill C, Ertay A, Li J, et al. Autophagy inhibition specifically promotes epithelial-mesenchymal transition and invasion in RAS-mutated cancer cells. Autophagy. 2019;15:886–99.
36. Chen DD, Cheng JT, Chandoo A, Sun XW, Zhang L, Lu MD, et al. microRNA-33a prevents epithelial-mesenchymal transition, invasion, and metastasis of gastric cancer cells through the Snail/Slug pathway. Am J Physiol Gastrointest Liver Physiol. 2019;317:G147–60.
37. Zeng S, Seifert AM, Zhang JQ, Cavnar MJ, Kim TS, Balachandran VP, et al. Wnt/beta-catenin Signaling Contributes to Tumor Malignancy and Is Targetable in Gastrointestinal Stromal Tumor. Mol Cancer Ther. 2017;16:1954–66.
38. Natalwala A, Spychal R, Tselepis C. Epithelial-mesenchymal transition mediated tumourigenesis in the gastrointestinal tract. World J Gastroenterol. 2008;14:3792–7.
39. Zhang MY, Wang J, Guo J. Role of Regenerating Islet-Derived Protein 3A in Gastrointestinal Cancer. Front Oncol. 2019;9:1449.
40. Shi H, Han J, Yue S, Zhang T, Zhu W, Zhang D. Prognostic significance of combined microRNA-206 and CyclinD2 in gastric cancer patients after curative surgery: A retrospective cohort study. Biomed Pharmacother. 2015;71:210–5.
41. Cappellesso R, Marioni G, Crescenzi M, Giacomelli L, Guzzardo V, Mussato A, et al. The prognostic role of the epithelial-mesenchymal transition markers E-cadherin and Slug in laryngeal squamous cell carcinoma. Histopathology. 2015;67:491–500.
42. Liu YN, Yin JJ, Abou-Kheir W, Hynes PG, Casey OM, Fang L, et al. MiR-1 and miR-200 inhibit EMT via Slug-dependent and tumorigenesis via Slug-independent mechanisms. Oncogene. 2013;32:296–306.

Tables

Due to technical limitations, the tables are only available as a download in the supplemental files section.

Figures

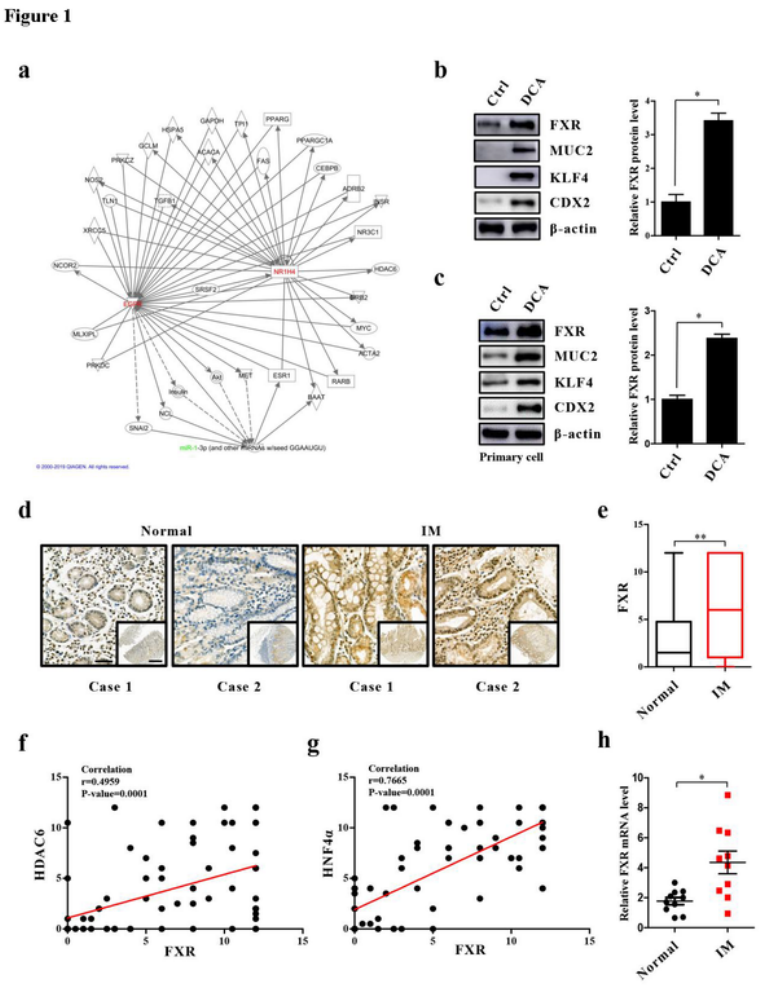

Figure 1

Upregulation of FXR in bile acids-stimulated intestinal metaplasia (IM) cells and tissues. a IPA analysis of bile acids receptor related to miR-1. b Left: Effects of DCA on the expression of FXR and intestinal markers (CDX2, MUC2, KLF4) in GES-1 cells. Cells were stimulated with DCA (100μM) or vehicle alone for 24 hours then the protein was extracted and subjected to western blot analysis for FXR, CDX2, MUC2, KLF4 and β-actin. β-actin levels were used as internal control in immunoblots. Right: Quantification of western blot analysis results were normalized as to β-actin. c Left: DCA (100μM) enhanced the protein levels of FXR and intestinal markers in primary gastric epithelial cells. Right: Quantification of western blot analysis results normalized as in figure 1B. d, e Immunohistochemical (IHC) staining for FXR in normal (n=24) and IM (n=80) tissues in microarrays. Scale bars: 100 μm; 500 μm (insets). f, g The correlation between FXR and HDAC6 or HNF4α in IM tissue. h The mRNA level of FXR in 10 pairs of matched human IM specimens. Each symbol represents mean value of an individual patient. Means±SEM of a representative experiment (n=3) performed in triplicates are shown. *$p<0.05$; **$p<0.01$. N.S., not significant.

Figure 2

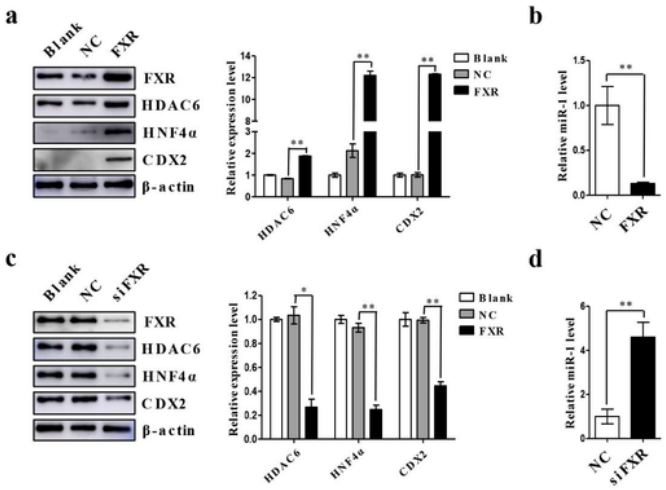

Figure 2

FXR regulates expression of intestinal markers positively in gastric cells. a Left: Western blot for intestinal markers and miR-1 targets in GES-1 cell infected with FXR expression vector. Right: Quantification of western blot analysis results were normalized as to β-actin. b MiR-1 expression in GES-1 cells was detected by qRT-PCR at 48 hours post-transfection. U6 was used as an internal control in qRT-PCR of miR-1. c Left: AGS cells were transfected with siFXR and intestinal markers were examined by immunoblots.

Right: quantification of western blot analysis results were normalized as figure 2A. d QRT-PCR was performed to examine miR-1 expression in AGS cells transfected with FXR specific siRNA. *p<0.05; **p<0.01. N.S., not significant.

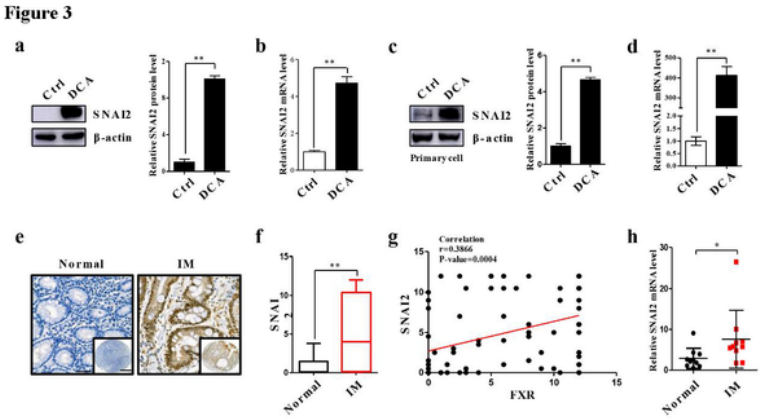

Figure 3

Overexpression of SNAI2 in IM cells. a GES-1 cells were treated as figure 1B. The protein level of SNAI2 was detected by immunoblots (Left) and the quantification of western blot analysis results was

normalized as to β-actin (Right). b The mRNA level of SNAI2 was examined in GES-1 cells after DCA by qRT-PCR. c, d Primary cultured cells were treated by DCA as in GES-1 cells, and SNAI2 was detected at protein and mRNA levels respectively. e Representative pictures of IHC staining for SNAI2 in normal and gastric IM tissues. Scale bars: 100 μm; 500 μm (insets). f Quantification of IHC staining for SNAI2. g The correlation between SNAI2 and FXR in IM specimens. h SNAI2 mRNA level in 10 pairs of matched human IM specimens. *p<0.05; **p<0.01. N.S., not significant.

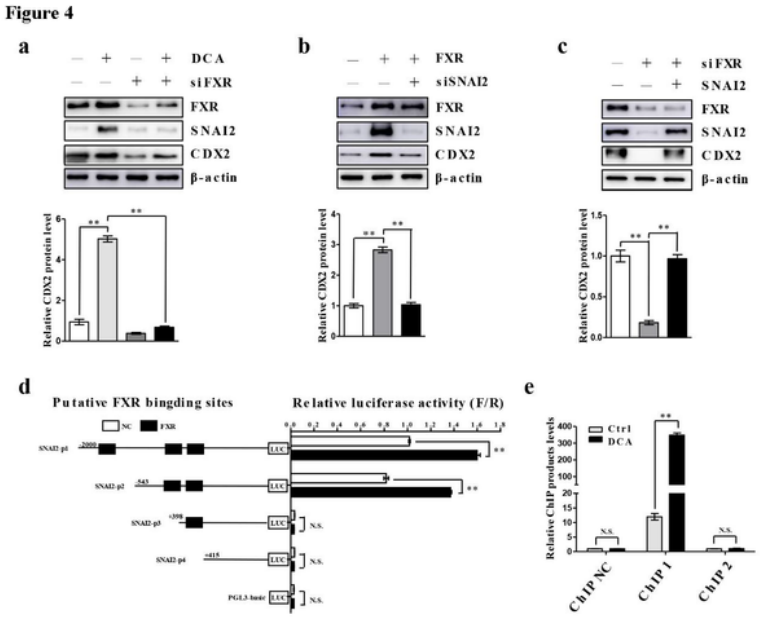

Figure 4

FXR positively regulates SNAI2 transcription. a Top: FXR inhibition reversed DCA-induced upregulation of SNAI2 and CDX2 in GES-1 cells. Bottom: Quantification of western blot analysis results was normalized as to β-actin. b GES-1 cells were treated with FXR expression vector and siSNAI2 simultaneously. Top: Downregulation of SNAI2 blocked the enhancement of CDX2 by FXR overexpression. Bottom: Quantification of western blot analysis results. c SNAI2 expression vector and siFXR were used to transfect AGS cells. Top: Upregulation of SNAI2 reversed the inhibition of CDX2 by FXR specific interference RNA. Bottom: Quantification of western blot analysis results. d Serially truncated CDX2 promoter constructs were cloned to pGL3-luciferase reporter plasmids and transfected into GES-1 cells. Four hours after transfection, cells were infected with FXR expression vector for 48 hours and the relative luciferase activities were determined. e QRT-PCR of the ChIP products validated the binding capacity of FXR to the SNAI2 promoter. *$p<0.05$; **$p<0.01$. N.S., not significant.

Figure 5

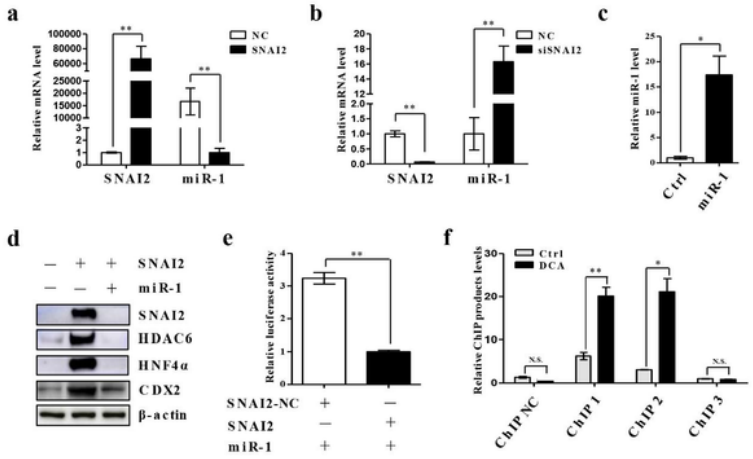

Figure 5

SNAI2 suppresses miR-1 transcriptionally in bile acids-induced IM cells. a, b QRT-PCR was performed to examine the mRNA- level of SNAI2 and miR-1 in GES-1 cells with SNAI2 overexpression or knockdown. c MiR-1 expression was enhanced by ago-miR-1 (100nM) in GES-1 cells. d Upregulation of intestinal markers and mir-1 targets induced by SNAI2 in GES-1 cells was abolished by miR-1 overexpression. e

SNAI2 inhibited miR-1 promoter activity in GES-1 cells. f ChIP assays validated the binding capacity of SNAI2 to the miR-1 promoter. *p<0.05; **p<0.01. N.S., not significant.

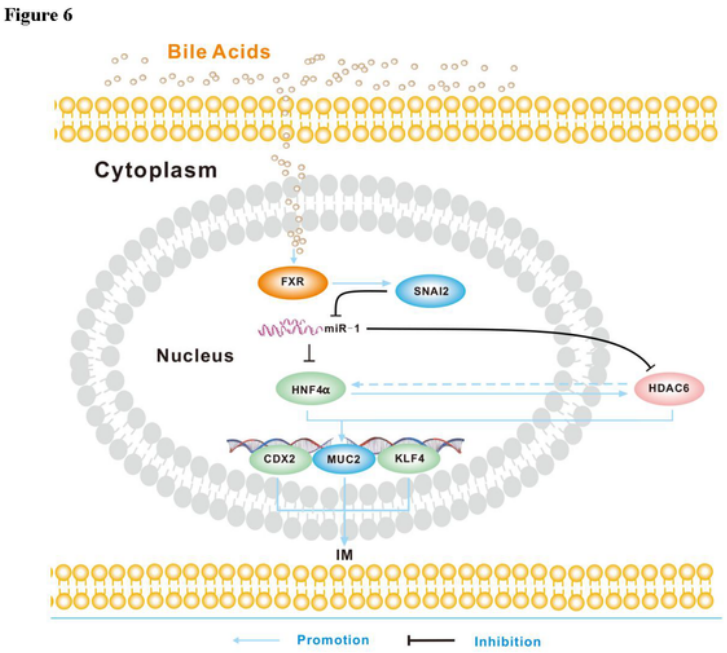

Figure 6

A new FXR/SNAI2/miR-1 signaling pathway promotes bile acids-induced gastric IM. Under the stimulation of bile acids, change in FXR gene expression increases the expression of SNAI2, which removes the inhibitory effect of miR-1 on HDAC6 and HNF4α. In particular, the upregulated HDAC6 and

HNF4α interact with each other, which further continuously promotes the upregulation of CDX2, KLF4, and MUC2, thus promoting the development of gastric IM.

Supplementary Files

This is a list of supplementary files associated with this preprint. Click to download.

- Supplementalfigure.pdf
- Table.pdf